MOLECULAR BIOLOGY

Mediator and RNA polymerase II clusters associate in transcription-dependent condensates

Won-Ki Cho[1]*, Jan-Hendrik Spille[1]*, Micca Hecht[1], Choongman Lee[1], Charles Li[2,3], Valentin Grube[1,4], Ibrahim I. Cisse[1]†

Models of gene control have emerged from genetic and biochemical studies, with limited consideration of the spatial organization and dynamics of key components in living cells. We used live-cell superresolution and light-sheet imaging to study the organization and dynamics of the Mediator coactivator and RNA polymerase II (Pol II) directly. Mediator and Pol II each form small transient and large stable clusters in living embryonic stem cells. Mediator and Pol II are colocalized in the stable clusters, which associate with chromatin, have properties of phase-separated condensates, and are sensitive to transcriptional inhibitors. We suggest that large clusters of Mediator, recruited by transcription factors at large or clustered enhancer elements, interact with large Pol II clusters in transcriptional condensates in vivo.

A conventional view of eukaryotic gene regulation is that transcription factors, bound to enhancer DNA elements, recruit coactivators such as the Mediator complex, which is thought to interact with RNA polymerase II (Pol II) at the promoter (*1*–*5*). This model is supported by a large body of molecular genetic and biochemical evidence, yet the direct interaction of Mediator and Pol II has not been observed and characterized in living cells (*6*). Using superresolution (*7*–*9*) and light-sheet imaging (*10*), we studied the organization and dynamics of endogenous Mediator and Pol II in live mouse embryonic stem cells (mESCs). We directly tested whether Pol II and Mediator interact in a manner consistent with condensate formation (*11*–*13*), quantitatively characterized their biophysical properties, and considered the implications of these observations for transcription regulation in living mammalian cells.

To visualize Mediator and Pol II in live cells, we generated mESC lines with endogenous Mediator and Pol II labeled with Dendra2, a green-to-red photoconvertible fluorescent protein (materials and methods and figs. S1 and S2). We performed live-cell superresolution imaging and found that Mediator forms clusters (Fig. 1A and fig. S3) with a range of dynamic temporal signatures. Mediator exists in a population of transient small (~100 nm) clusters (Fig. 1B) with an average lifetime of 11.1 ± 0.9 s (mean ± SEM from 36 cells) (Fig. 1G), comparable to that of transient Pol II clusters observed in this study (Fig. 1, D, E, and H) and previously in differentiated cell types (*14*, *15*). In addition, we observed that both Mediator and Pol II form a population of large (>300 nm) clusters (~14 per cell), each comprising ~200 to 400 molecules, that are temporally stable (lasting the full acquisition window of the live-cell superresolution imaging) (Fig. 1, C and F to H, and figs. S4 to S6).

We tested the extent to which these clusters depend on the stem cell state. The mESCs were subjected to a protocol (*16*) to differentiate them into epiblastlike cells (EpiLCs) within 24 h (materials and methods and fig. S7). Differentiation had no apparent effect on the population of transient clusters, consistent with previous observations that transient clusters persist in differentiated cell types (*14*, *15*). However, both the size and the number of stable clusters decreased along the course of differentiation (fig. S8), suggesting that these stable clusters are prone to change as cells differentiate.

We focused on the stable clusters of Mediator and Pol II and investigated whether they are colocalized. We generated mESCs with endogenous Mediator and Pol II tagged with JF646-HaloTag (*15*, *17*) and Dendra2, respectively (materials and methods and figs. S1 and S2). Direct imaging of both JF646-Mediator (Fig. 2A) and Dendra2–Pol II (Fig. 2B) showed bright spots of large accumulations in the nucleus, which corresponded to stable Pol II clusters according to subsequent superresolution imaging of Dendra2–Pol II in the same nuclei (Fig. 2C). The same observations were made with Dendra2-Mediator (fig. S9). Of 143 Mediator clusters imaged by dual-color light-sheet imaging (Fig. 2, D to F), 129 (90%) had a colocalizing Pol II cluster (Fig. 2, G and H; materials and methods; and fig. S9). We conclude that these Mediator and Pol II clusters colocalize in live mESCs.

Previous studies have shown that high densities of Mediator are located at enhancer clusters called super-enhancers (SEs) and that some are

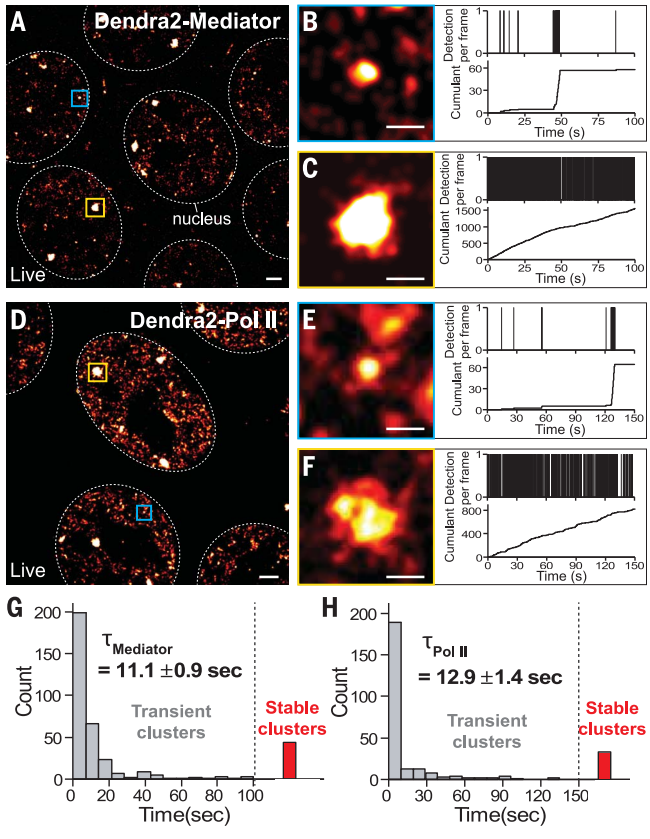

Fig. 1. Mediator and Pol II form transient and stable clusters in living mESCs. (**A**) A superresolution image of endogenous Mediator labeled with Dendra2 in living mESCs. (**B** and **C**) Representative superresolved images of transient and stable Mediator clusters and corresponding time-correlated photoactivation localization microscopy (tcPALM) traces. (B) and (C) correspond to areas boxed in blue and yellow, respectively, in (A). (**D**) Superresolution image of endogenous Pol II labeled with Dendra2 in living mESCs. (**E** and **F**) Representative superresolution images of transient and stable Pol II clusters and corresponding tcPALM traces. (E) and (F) correspond to areas boxed in blue and yellow, respectively, in (D). (**G** and **H**) Lifetime distributions of Mediator and Pol II clusters, respectively. Scale bars, 1 μm in (A) and (D) and 500 nm in (B), (C), (E), and (F).

[1]Department of Physics, MIT, Cambridge, MA 02139, USA. [2]Department of Biology, MIT, Cambridge, MA 02139, USA. [3]Whitehead Institute for Biomedical Research, Cambridge, MA 02139, USA. [4]Department of Physics, LMU Munich, Geschwister Scholl Platz 1, 80539 Munich, Germany.
*These authors contributed equally to this work.
†Corresponding author. Email: icisse@mit.edu

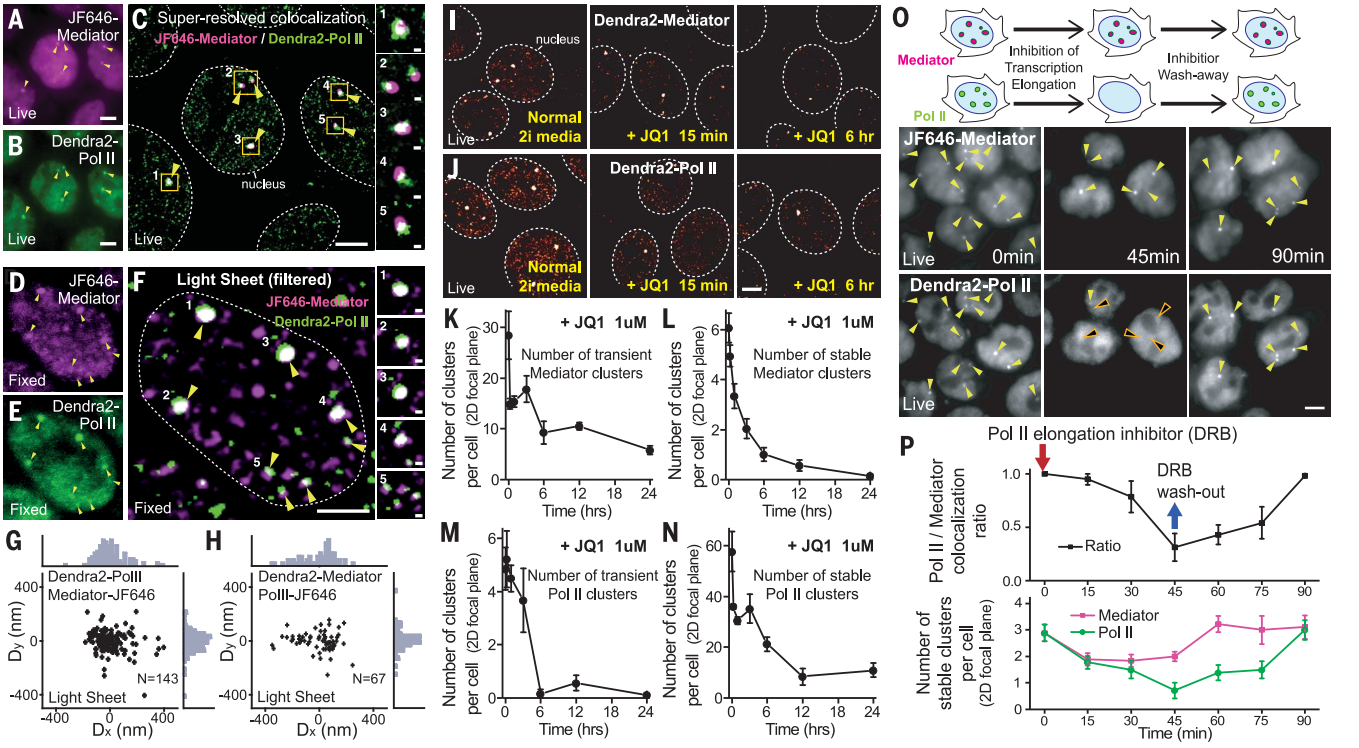

Fig. 2. Mediator and Pol II clusters colocalize in a transcription-dependent manner. Live-cell direct images of (**A**) JF646-Mediator and (**B**) Dendra2–Pol II. Yellow arrowheads indicate stable clusters. (**C**) Super-resolution image of Dendra2–Pol II overlaid with a background-subtracted JF646-Mediator image. Insets 1 to 5 show Mediator and Pol II colocalization in clusters. (**D**) JF646-Mediator and (**E**) Dendra2–Pol II maximum-intensity projections of a fixed cell imaged by lattice light-sheet microscopy. (**F**) Overlay of background-subtracted images. Yellow arrowheads indicate clusters identified in the Dendra2–Pol II channel. (**G**) Scatter plot of the distance *D* from a Dendra2–Pol II cluster to the nearest JF646-Mediator cluster (n = 143 clusters). Histograms outside the scatter plot show the distances along the *x* and *y* axes. (**H**) Same analysis for clusters identified in the Dendra2-Mediator channel (n = 67). (**I** and **J**) Superresolution images of Dendra2-Mediator and Dendra2–Pol II under normal conditions (left) and after 15 min (middle) or 6 hours (right) of incubation in 1 μM JQ1. (**K** and **M**) The number of transient Mediator and Pol II clusters per cell in a 2D focal plane as a function of time after JQ1 addition. (**L** and **N**) The number of stable Mediator and Pol II clusters per cell in a 2D focal plane. n = 17 to 25 cells and n = 14 to 24 cells at each JQ1 time point for Mediator and Pol II, respectively. (**O**) DRB treatment and washout experiments. DRB (100 μM) was added at 0 min and washed away after 45 min. Arrowheads indicate stable clusters identified in the JF646-Mediator channel. Black arrowheads in the middle panel (bottom) indicate Mediator clusters that did not colocalize with Pol II clusters. (**P**) Ratio (top) and absolute number (bottom) of clusters detected in the Pol II and Mediator channels per cell in a 2D focal plane. Nine to 15 cells were analyzed for each DRB incubation time point. The red arrow indicates the addition of DRB, and the blue arrow indicates DRB washout. Scale bars, 2 μm in overview images and 200 nm in insets.

disrupted by loss of the BET (bromodomain and extraterminal family) protein BRD4, which is a cofactor associated with Mediator (*18*, *19*). We found that treatment of mESCs with JQ1, a drug that causes loss of BRD4 from enhancer chromatin, dissolved transient and stable clusters of both Mediator and Pol II clusters (Fig. 2, I to N, and fig. S10).

After transcription initiation, Pol II transcribes a short distance (~100 base pairs), pauses, and is released to continue elongation when phosphorylated by CDK9 (*20*). We hypothesized that inhibition of CDK9 might selectively affect the Pol II stable clusters. We observed that upon incubation with DRB (5,6-dichloro-1-beta-D-ribofuranosylbenzimidazole), Pol II stable clusters dissolved but Mediator stable clusters remained (Fig. 2O). Quantification of Mediator–Pol II colocalization revealed that incubation with DRB progressively decreased the fraction of Mediator stable clusters that colocalized with Pol II (Fig. 2P). This effect could be reversed when DRB was washed out; the colocalization fraction recovered completely. These results imply that the association between Mediator and Pol II clusters may be hierarchical, with upstream enhancer recruitment controlling both clusters but downstream transcription inhibition selectively affecting Pol II clusters.

We characterized the long-term dynamics of stable clusters by using lattice light-sheet imaging in live mESCs (movies S1 and S2). We observed that clusters can merge upon contact (Fig. 3, A to D, and movies S1 and S2). The time scale of coalescence was very rapid, comparable to our full volumetric acquisition frame rate (15-s time interval). The added-up intensity of the two precursor clusters was close to that of the newly merged cluster (Fig. 3E and fig. S11). These biophysical dynamics are reminiscent of those of biomolecular condensates in vivo (*21*).

In addition to coalescence, in vivo condensates had rapid turnover of the molecular components, as shown by fast recovery in fluorescence recovery after photobleaching (FRAP) assays, and were sensitive to a nonspecific aliphatic alcohol, 1,6-hexanediol (*21*). Our FRAP analyses of clusters revealed very rapid dynamics and turnover of their components: 60% of the Mediator and 90% of Pol II components were exchanged within ~10 s within clusters (Fig. 3, F to H). Moreover, the treatment of mESCs with 1,6-hexanediol resulted in the gradual dissolution of both Mediator and Pol II clusters (Fig. 3, I to K, and fig. S12). Together, these results suggest that the stable clusters are in vivo condensates of Mediator and Pol II.

We hypothesized that a phase separation model with induced condensation at the recruitment step of Mediator to enhancers would qualitatively account for the observations in this study (*22*). The model implies that the condensates are chromatin associated and colocalize with enhancer-controlled active genes. We therefore tested these two specific implications. We tracked the diffusion dynamics of Mediator clusters by computing their mean squared displacement as a function of time (n = 6 cells). On short time scales, the cluster motion was subdiffusive,

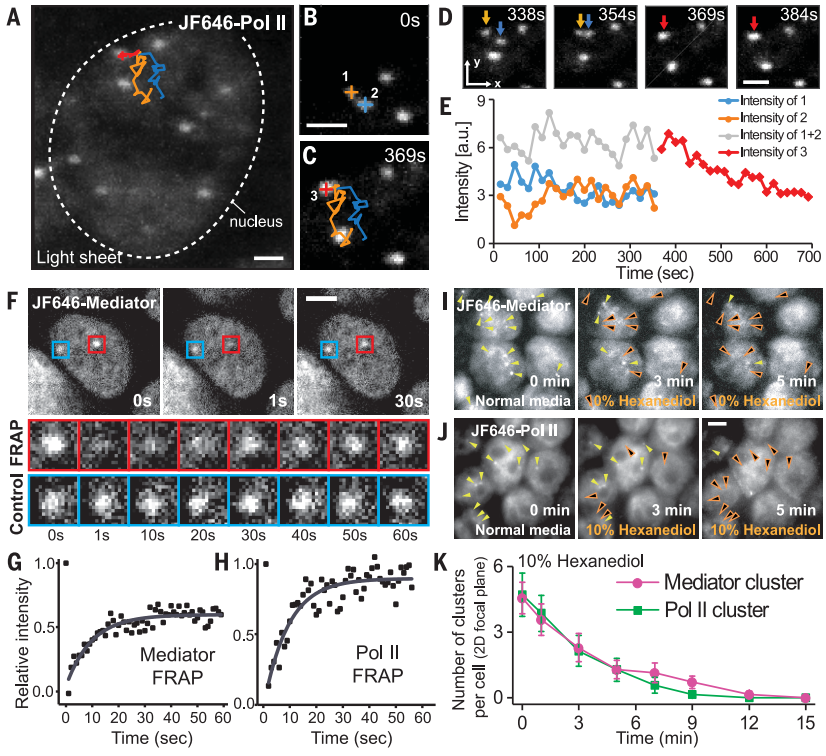

Fig. 3. Mediator and Pol II form condensates that coalesce, recover in FRAP, and are sensitive to hexanediol. (**A** to **E**) Cluster fusion. (A) Maximum-intensity projection of a live cell imaged by lattice light-sheet microscopy. Trajectories of two clusters are indicated. (B and C) Clusters observed at 0 s and fusing at 369 s. (D) Individual time points around the fusion event. Orange and blue arrows indicate the precursor clusters, and the red arrows indicate the fused cluster. (E) Time course of the cluster intensities. a.u., arbitrary units. (**F** to **H**) FRAP analysis of clusters. (F) (Top) Images of a JF646-Mediator cell before (0 s) (left), immediately after (1 s) (middle), and 30 s after (right) bleaching. The red box indicates the position of the cluster on which the FRAP beam was focused. The blue box indicates an unbleached control locus. (Bottom) Cropped images as a function of time for both loci. (G) The normalized recovery curve for Mediator (n = 9 cells) yielded a recovery fraction of 60% during the 60-s observation, with a half-recovery time of 10 s. (H) FRAP analysis of JF646–Pol II (n = 3 cells) yielded 90% recovery, with an identical half-recovery time of 10 s. (**I** and **J**) Treatment with 10% hexanediol (v/v) gradually dissolved clusters of JF646-Mediator (I) and JF646–Pol II (J). Maximum-intensity projections of epifluorescence z stacks are shown. Yellow arrowheads indicate clusters identified at 0 min. Black arrowheads indicate clusters that disappeared. (**K**) Average number of clusters per cell (single 2D focal plane) observed in direct imaging as a function of time after hexanediol addition (n = 14 cells for JF646-Mediator, and n = 14 cells for JF646–Pol II). Scale bars, 1 μm (A to D) and 5 μm (F and J).

with an exponent $\alpha = 0.40 \pm 0.12$ (best fit ± SEM) (fig. S13). This is the same exponent found in the subdiffusional behavior of chromatin loci in eukaryotic cells (*23*–*27*). We also observed the same diffusional parameters when tracking a chromatin locus labeled by dCas9-based chimeric array of guide RNA oligonucleotides (CARGO) in mESCs (fig. S13) (*23*). We concluded that clusters diffuse like chromatin-associated domains.

We hypothesized that clusters were in close physical proximity to actively transcribed genes that can be visualized by global run-on nascent RNA labeling with ethynyl uridine (EU) (fig. S14). The run-on results showed that 2 min after DRB washout, virtually all Mediator clusters observed were proximal or overlapping with nascent RNA accumulations, as imaged by Click labeling of EU in fixed cells (fig. S14). We also employed the MS2 endogenous RNA labeling system (*15*, *28*) (materials and methods and fig. S15) to investigate whether active transcription could be observed at *Esrrb*, one of the top SE-controlled genes in mESCs (*29*) (Fig. 4A). We observed bright foci consistent with nascent MS2-labeled gene loci and confirmed the gene loci by dual-color RNA fluorescence in situ hybridization (FISH) targeting the MS2 sequence and intronic regions of *Esrrb* (fig. S16). Intronic FISH on 125 *Esrrb* loci from 82 fixed cells showed that 93% of *Esrrb* loci had a stable Mediator cluster nearby (within 1 μm) but only ~22% of the loci colocalized with a stable Mediator cluster, suggesting that the Mediator-bound enhancer only occasionally colocalizes with the gene (fig. S17). The variability in colocalization may be explained by a dynamic "kissing" model, where a distal Mediator cluster colocalizes with the gene only at certain time points (Fig. 4A).

By dual-color three-dimensional (3D) live-cell imaging with lattice light-sheet microscopy, we found that some Mediator clusters were up to a micrometer away from the active *Esrrb* gene locus but in some instances directly colocalized with the gene (Fig. 4, B and C). In addition, we directly observed the dynamic interaction between Mediator clusters and the gene locus, supporting the dynamic kissing model (Fig. 4, D and E; fig. S18; and movie S3). Tracking of loci in all six cells indicated that colocalization below our resolution limit of 300 nm occurred at ~30% of the time points (Fig. 4F). However, even when they were not overlapping, the Mediator cluster and the gene loci moved as a pair through the nucleus (movie S3), consistent with two adjacent regions anchoring to the same underlying chromatin domain. We propose that Mediator clusters form at the *Esrrb* SE and then interact occasionally and transiently with the transcription apparatus at the *Esrrb* promoter.

We have found that Mediator and Pol II form large stable clusters in living cells and have shown that these clusters have properties expected for biomolecular condensates. The condensate properties were evident through coalescence, rapid recovery in FRAP analysis, and sensitivity to hexanediol. In a model of phase separation on the basis of scaffold-client relationships (*30*), it is possible that enhancer-associated Mediator forms a condensate and provides a "scaffold" for "client" RNA Pol II molecules. The model we propose whereby large Mediator clusters at

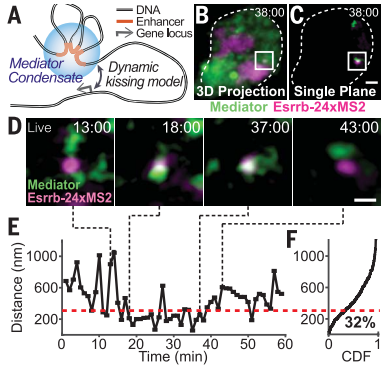

Fig. 4. Mediator clusters dynamically kiss actively transcribing SE-controlled genes. (**A**) Illustration of the working model describing cluster-kissing interaction with a gene locus. (**B**) Maximum-intensity projection of a cell imaged by using lattice light-sheet microscopy showing colocalization of a JF646-Mediator cluster with the actively transcribing *Esrrb* gene locus marked by MS2-tagged RNA (white box). (**C**) Single plane from the z stack after background subtraction. (**D**) Snapshot images of a Mediator cluster near the actively transcribing *Essrb* gene locus. Time points listed in (B) to (D) indicate minutes after the start of acquisition. Scale bars, 2 μm in (B) and (C) and 500 nm in (D). (**E**) Plot of the centroid-to-centroid distance from the gene locus to the nearest cluster as a function of time. (**F**) Cumulative distribution of distances from the *Esrrb* locus to the nearest Mediator cluster pooled from six cells (291 time points). The red dashed line in (E) and (F) indicates the colocalization threshold (300 nm). CDF, cumulative distribution function.

enhancers transiently kiss the transcription apparatus at promoters has a number of implications for gene control mechanisms. The presence of large Mediator clusters at some enhancers may allow Mediator condensates to contact the transcription apparatus at multiple gene promoters simultaneously. The large size of the Mediator clusters may also mean that the effective distance of the enhancer-promoter DNA elements can be in the same order as the size of the clusters (>300 nm), larger than the distance requirement for direct contact. We speculate that such clusters may help explain gaps of hundreds of nanometers that are found in previous studies measuring distances between functional enhancer-promoter DNA elements. Such cluster sizes also imply that some long-range interactions could go undetected in DNA interaction assays that depend on much closer physical proximity of enhancer and promoter DNA elements.

REFERENCES AND NOTES

1. P. J. Robinson *et al*., *Cell* **166**, 1411–1422.e16 (2016).
2. R. D. Kornberg, *Trends Biochem. Sci.* **30**, 235–239 (2005).
3. C. T. Ong, V. G. Corces, *Nat. Rev. Genet.* **12**, 283–293 (2011).
4. K. M. Lelli, M. Slattery, R. S. Mann, *Annu. Rev. Genet.* **46**, 43–68 (2012).
5. B. L. Allen, D. J. Taatjes, *Nat. Rev. Mol. Cell Biol.* **16**, 155–166 (2015).
6. M. Levine, C. Cattoglio, R. Tjian, *Cell* **157**, 13–25 (2014).
7. S. T. Hess, T. P. Girirajan, M. D. Mason, *Biophys. J.* **91**, 4258–4272 (2006).
8. M. J. Rust, M. Bates, X. Zhuang, *Nat. Methods* **3**, 793–796 (2006).
9. E. Betzig *et al*., *Science* **313**, 1642–1645 (2006).
10. B. C. Chen *et al*., *Science* **346**, 1257998 (2014).
11. D. Hnisz, K. Shrinivas, R. A. Young, A. K. Chakraborty, P. A. Sharp, *Cell* **169**, 13–23 (2017).
12. T. Fukaya, B. Lim, M. Levine, *Cell* **166**, 358–368 (2016).
13. Z. Liu *et al*., *eLife* **3**, e04236 (2014).
14. I. I. Cisse *et al*., *Science* **341**, 664–667 (2013).
15. W. K. Cho *et al*., *eLife* **5**, e13617 (2016).
16. C. Buecker *et al*., *Cell Stem Cell* **14**, 838–853 (2014).
17. J. B. Grimm *et al*., *Nat. Methods* **12**, 244–250 (2015).
18. P. Filippakopoulos *et al*., *Nature* **468**, 1067–1073 (2010).
19. J. Lovén *et al*., *Cell* **153**, 320–334 (2013).
20. N. F. Marshall, D. H. Price, *Mol. Cell. Biol.* **12**, 2078–2090 (1992).
21. Y. Shin, C. P. Brangwynne, *Science* **357**, eaaf4382 (2017).
22. B. R. Sabari *et al*., *Science* **361**, eaar3958 (2018).
23. B. Gu *et al*., *Science* **359**, 1050–1055 (2018).
24. J. R. Chubb, S. Boyle, P. Perry, W. A. Bickmore, *Curr. Biol.* **12**, 439–445 (2002).
25. J. S. Lucas, Y. Zhang, O. K. Dudko, C. Murre, *Cell* **158**, 339–352 (2014).
26. V. Dion, S. M. Gasser, *Cell* **152**, 1355–1364 (2013).
27. S. C. Weber, A. J. Spakowitz, J. A. Theriot, *Phys. Rev. Lett.* **104**, 238102 (2010).
28. E. Bertrand *et al*., *Mol. Cell* **2**, 437–445 (1998).
29. W. A. Whyte *et al*., *Cell* **153**, 307–319 (2013).
30. S. F. Banani, H. O. Lee, A. A. Hyman, M. K. Rosen, *Nat. Rev. Mol. Cell Biol.* **18**, 285–298 (2017).

ACKNOWLEDGMENTS

We thank L. D. Lavis (HHMI, Janelia) and J. Grimm (HHMI, Janelia) for the gift of the JF646-Halo dyes and E. Calo (MIT) for the wild-type R1 cells and differentiation protocol. We thank J. Wysocka (Stanford) for the CARGO material. We thank R. Young (MIT) and members of the Young, Sharp, and Chakraborty groups (MIT) for helpful discussions and R. Young and J. Gore (MIT) for helpful comments on the manuscript. We acknowledge the students of the Cissé lab rotation in the 2017 Marine Biology Laboratory physiology course for participation in early aspects of Dendra2–Pol II characterization in mESCs and J. O. Andrews for assistance with the quantitative superresolution analysis software. The lattice light-sheet microscope was home built in the Cissé lab at MIT Physics under license from HHMI, Janelia Research Campus, and we thank E. Betzig (HHMI, Janelia) and W. Legant (HHMI, Janelia) for their critical support in the process. FRAP experiments were performed at the W. M. Keck Microscopy Facility at the Whitehead Institute. We thank L. Boyer for help with stem cell culture. **Funding:** This work was supported primarily by the NIH director's New Innovator award (DP2CA195769 to I.I.C.) and also by the Pew Charitable Trusts through the Pew Biomedical Scholars Program grant (to I.I.C.). I.I.C. is also supported by the NIH 4D Nucleome through NOFIC. J.-H.S. is supported by a postdoctoral fellowship from the German Research Foundation (DFG, SP1680/1-1). **Author contributions:** W.-K.C., J.-H.S., and I.I.C. conceived of and designed the study; W.-K.C. and J.-H.S. performed experiments and analyzed data with help from M.H., C.Le., and V.G.; M.H. cloned CRISPR repair templates and single-guide RNA plasmids and genotyped cell lines; C.Li conducted and analyzed the Western blot and chromatin immunoprecipitation sequencing (ChIP-seq) assays; W.-K.C., J.-H.S., and I.I.C. wrote the manuscript with input from all coauthors; and I.I.C. supervised all aspects of the project. **Competing interests:** The authors declare that they have no competing interests. **Data and materials availability:** All data and materials will be provided upon reasonable request to the corresponding author. ChIP-seq datasets generated in this study have been deposited in the Gene Expression Omnibus under accession number GSE115436. Other data described in the text are presented in the supplementary materials.

SUPPLEMENTARY MATERIALS

www.sciencemag.org/content/361/6400/412/suppl/DC1
Materials and Methods
Figs. S1 to S18
Tables S1 to S10
References (*31*–*43*)
Movies S1 to S3

6 November 2017; resubmitted 17 April 2018
Accepted 11 June 2018
Published online 21 June 2018
10.1126/science.aar4199

Science

Mediator and RNA polymerase II clusters associate in transcription-dependent condensates

Won-Ki Cho, Jan-Hendrik Spille, Micca Hecht, Choongman Lee, Charles Li, Valentin Grube and Ibrahim I. Cisse

Science **361** (6400), 412-415.
DOI: 10.1126/science.aar4199originally published online June 21, 2018

Phase separation and gene control

Many components of eukaryotic transcription machinery—such as transcription factors and cofactors including BRD4, subunits of the Mediator complex, and RNA polymerase II—contain intrinsically disordered low-complexity domains. Now a conceptual framework connecting the nature and behavior of their interactions to their functions in transcription regulation is emerging (see the Perspective by Plys and Kingston). Chong *et al.* found that low-complexity domains of transcription factors form concentrated hubs via functionally relevant dynamic, multivalent, and sequence-specific protein-protein interaction. These hubs have the potential to phase-separate at higher concentrations. Indeed, Sabari *et al.* showed that at super-enhancers, BRD4 and Mediator form liquid-like condensates that compartmentalize and concentrate the transcription apparatus to maintain expression of key cell-identity genes. Cho *et al.* further revealed the differential sensitivity of Mediator and RNA polymerase II condensates to selective transcription inhibitors and how their dynamic interactions might initiate transcription elongation.

Science, this issue p. eaar2555, p. eaar3958, p. 412; see also p. 329